

Study on Abrasive Wear of Brake Pad in the Large-megawatt Wind Turbine Brake Based on Deform Software

Shengfang Zhang, Qiang Hao, Zhihua Sha, Jian Yin, Fujian Ma and Yu Liu*

School of Mechanical Engineering, Dalian Jiaotong University, Dalian, China 116028

zsf@djtu.edu.cn, haoqiang983@163.com, shirlysha@hotmail.com,
yinjian429578951@sina.com, mafujianyx@163.com, liuyu_ly12@126.com*

Abstract. For the friction and wear issues of brake pads in the large-megawatt wind turbine brake during braking, this paper established the micro finite element model of abrasive wear by using Deform-2D software. Based on abrasive wear theory and considered the variation of the velocity and load in the micro friction and wear process, the Archard wear calculation model is developed. The influence rules of relative sliding velocity and friction coefficient in the brake pad and disc is analysed. The simulation results showed that as the relative sliding velocity increases, the wear will be more serious, while the larger friction coefficient lowered the contact pressure which released the wear of the brake pad.

1. Introduction

In recent years, the wind turbine industry develops rapidly, which increases the installed capacity of wind turbine. For the high-speed and heavy-load condition of the large-megawatt wind turbine brake, friction of the brake pad/disc causes wear in the brake system which leads to many problems indirectly. It is important to study the friction and wear of the brake pad/disc. Stadler et al. study the tribology behaviour of wear between metal sintered brake and C/C-SiC composite disc[1]. Cho et al. discuss the effect of interface transfer layer of metal-based brake and gray cast iron brake disc on the tribology properties[2]. For rough friction surface, Liu et al. analyse the maximum flash temperature, the contact pressure and real contact area of the rough surface by using the finite element method[3]. Bogdanvoich et al. research the temperature field distribution of the rough surface in the sliding friction process by experiments[4]. Straffelini et al. and Mikael et al. study the internal mechanism of the change of the contact surface of the friction material and the change of the wear rate with the enhanced particle size in the high speed state[5-6]. Uyyuru et al. investigate the effect of strengthening the volume fraction and size distribution on the friction and wear properties of aluminium matrix composites[7]. Zhou et al. take non-smooth surface of circular pits as an example, analyse the wear process of non-smooth surface pits with different diameters and depths[8].

The above researches mainly study the influence of friction material and surface morphology on the friction and wear, and do not analyse the wear rules in abrasion quantitatively. Based on the abrasive wear in the friction mechanism, the Archard wear model is improved in this paper. The abrasive wear model of the large-megawatt wind turbine brake pad is carried out with the finite element analysis by Deform-2D software. The effects of relative sliding velocity and friction coefficient on abrasive wear of brake pad are presented. And the wear rules of the modified Archard wear model are obtained.



2. Calculation model of abrasive wear

For the high-speed and heavy-load condition of the large-megawatt wind turbine brake, based on abrasive wear theory, the generalized linear wear model of Archard is improved, and the variation of the wear depth calculation model can be obtained. It is assumed that the wear depth is related to the relative sliding velocity and the interface pressure, which means that the wear depth can be calculated by the relative sliding velocity and the interface pressure in every unit time. The concrete Archard wear model is as follow[9]:

$$V = K \frac{PL}{H} \quad (1)$$

In which, V is the wear volume, P is the normal pressure of the contact surface in the brake pad/disc, L is the relative sliding distance between abrasive and brake pad, H is the hardness, K is the dimensionless wear coefficient which varies from 10^{-2} to 10^{-7} according to different contact conditions.

However, any interface in the actual project is not smooth absolutely. The actual contacting area is related to the actual interface of the micro-morphology, the point of stress on the brake pad/disc and the wear depth of the interface are closely related to the wear state. The stress changes with the wear depth of the interface, which leads to the variation of the wear degree. Therefore, for a concrete contact point of a simulated wear depth, the original Archard model is no longer applicable. In this case, the Archard model needs to be modified in the specific wear area, which means the stress σ and the relative sliding velocity v are seen as influencing factors. The concrete equation is as follow:

$$h = \frac{K}{H} \int_0^t [v(t)\sigma(t)]dt \quad (2)$$

A single wear is made up of intervals m , and the wear depth is:

$$h_{j,n} = \sum_{i=1}^m \Delta h_{j,n} = \sum_{i=1}^m \frac{K}{H} v_{j,n} \sigma_{j,n} \Delta t \quad (3)$$

In which, j is the iteration number, n is the contact points number.

So the total wear depth W is:

$$W = \sum_{j=1}^k h_{j,n} \quad (4)$$

In which, k is the total iteration number.

According to Equation (4), the quantitative results of abrasive wear can be obtained. The concrete process is divided into two steps: 1) the relative sliding velocity and the stress data which belong to the wear stage are extracted from the contact point. 2) those data are divided and put into the equation to solve.

3. Establishment of abrasive wear finite element model

Based on abrasive wear theory, the micro finite element model of abrasive wear is established by using Deform-2D software. The cone abrasive on the brake pad is $2\mu\text{m}$, and the radius of the bottom fillet is $0.5\mu\text{m}$. The material is copper-based powder metallurgy. The property is set to be rigid. The brake pad takes $20\mu\text{m} \times 5\mu\text{m}$ with rectangle. The material is 45 steel, and the property is set to be plastic. The specific parameters of the material are shown in Table 1.

Table 1. Material parameters of abrasive and brake pad.

	Density (kg/m^3)	Thermal conductivity [$\text{W}/(\text{m} \cdot \text{K})$]	Elastic Modulus (GPa)	Poisson's ratio	Linear expansion coefficient	Specific heat capacity [$\text{J}/(\text{kg} \cdot \text{K})$]
Abrasive	5250	30	5.2	0.3	1.5×10^{-11}	550
Brake pad	7250	57	138	0.28	1.085×10^{-5}	450

The model can be meshed, and the volume of the deformity body can be compensated by using the adaptive meshing technique. The contact area of the brake pad/disc is grid-encrypted, and the grid is sparse away from the analysed area. The grid model is shown in Figure 1.

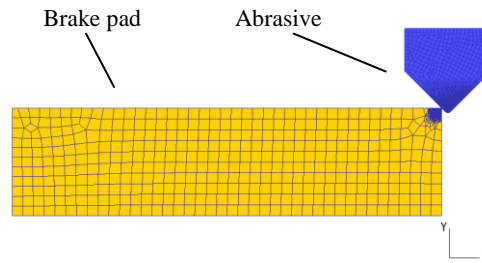


Figure 1. Finite element model of abrasive wear of brake pad.

Regarding to the boundary conditions, the abrasive and the brake pad should be set separately. The full restrain of the brake pad is used to restrain the freedom degree of the bottom unit. The relative motion in the X, Y and Z directions are 0. Abrasive needs to be given an X negative direction of the speed. It is assumed that the heat exchange coefficient between the abrasive and the surface of the brake pad is 45 N/sec/mm/C, and the friction coefficient is assumed unchanged with the temperature. Set the environment temperature to 20°C. In the simulation process, shear failure model and tensile failure model are adopted. The shear model is based on the average plastic strain value at the cell node.

The failure is assumed to occur when the destructive parameter $\omega_1 \geq 1$. The destructive parameter ω_1 is defined as:

$$\omega_1 = \sum \left(\frac{\Delta \varepsilon^{PL}}{\overline{\Delta \varepsilon^{PL}}} \right) \tag{5}$$

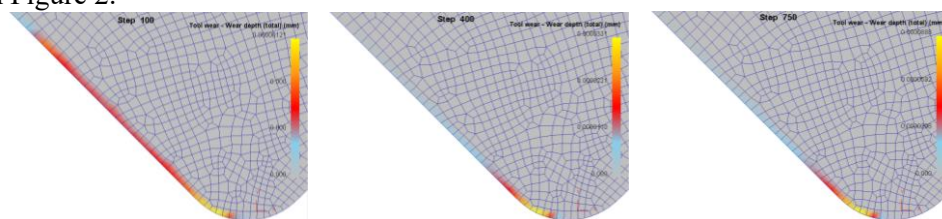
In which, $\Delta \varepsilon^{PL}$ is the increment of the average plastic strain, $\overline{\Delta \varepsilon^{PL}}$ is the failure strain.

When the node stress reaches the shear failure criterion, the corresponding material fails at this point. The shear failure criterion is chosen, and the wear equation is used to deduce the modified equation of the Archard wear model. Because the wear is a cumulative process, it takes a long time to work continuously to observe the wear rules. Therefore, to increase the number of simulation steps in the simulation process is needed, the number of simulation steps is controlled in 750 steps, and the data is read and saved with every 10 steps, meanwhile the international unit system is selected. The simulation mode is heat transfer and deformation. For the consideration of the flow stress in the disc material affected by strain, strain rate and temperature, the conjugate gradient method is chosen to be the iterative method.

4. Simulation results and analysis

4.1. Simulation results of wear nephogram analysis

The nephogram of abrasive wear with relative sliding velocity $v=10\text{m/s}$ and friction coefficient $\mu=0.60$ is shown in Figure 2.



(a) step 100 (b) step 300 (c) step 750
Figure 2. Nephogram of the abrasive wear in different time.

Abrasive wear is a microscopic wear process, and the wear is also a long cumulative process. It can be seen from Figure 2(a) that at the interface of friction, the wear occurs. The abrasive bottom interface wear is more serious, away from the bottom of the surface the wear is less. In the initial stage of wear, the abrasive wear depth is very small, the wear is relatively minor. It is because the abrasive particles and brake pad just come into contact, the contact surface temperature and contact stress are relatively small, and the corresponding wear is relatively small. From Figure 2(b), (c) and (d), it can be found that the wear of the contact surface accumulates and reaches a steady stage gradually with the simulation progresses. Due to the relative sliding velocity and the contact stress, the maximum wear depth reaches $h=8.88\times 10^{-5}$ mm at the 750th step.

4.2. Effect of relative sliding velocity on abrasive wear

Relative sliding velocity is one of the factors that affects wear. Different relative sliding velocity has a great impact on wear, especially in the high-velocity and heavy-load. The greater relative sliding velocity leads to the higher temperature. Therefore, a single variable method is used to simulate, when $\mu=0.60$ and $v=6\text{m/s}$, $v=8\text{m/s}$ and $v=10\text{m/s}$ respectively.

The temperature of the interface can be obtained directly from the post-processing results of Deform-2D. At the 750th step, the maximum temperature of the current sub-step is extracted every 10 steps. The interface temperature curve can be obtained at different relative sliding velocity, as shown in Figure 3.

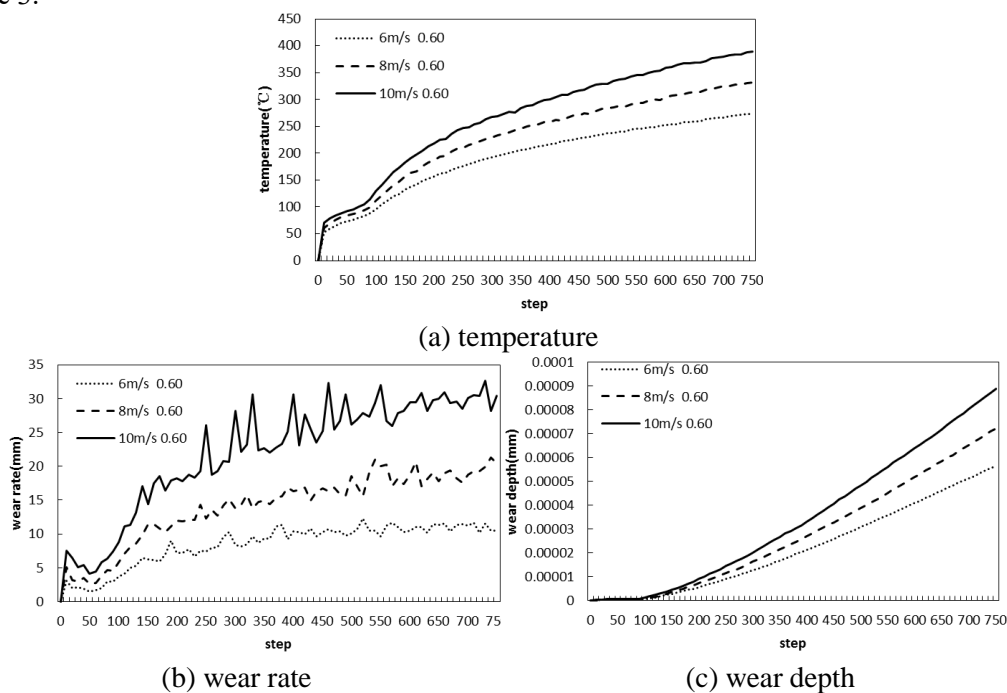


Figure 3. Chart of parameters with different relative sliding velocity.

It can be seen from Figure 3(a) that the interface temperature from the 1st step to the 750th step increases with the wear. At the 750th step, the max interface temperature is at 273.399°C when $v=6\text{m/s}$. When the relative sliding velocity increases $v=10\text{m/s}$, the max temperature of the interface is at 389.344°C. It can be found that the relative sliding velocity v increases, the interface temperature also increases correspondingly. Mainly because of the relative sliding velocity increasing, the unit time friction and material deformation are generated by the heat increasing, abrasive and brake pad are pressed state, the interface of the heat generated is difficult to spread, the temperature increases correspondently.

Figure 3(b) and (c) show that the relationship between the relative sliding velocity and the wear rate and wear depth. The wear rate of the different relative sliding rate trending and the max wear

respectively can be found in Figure 4. It can be seen from Figure 3(b) that the wear rate of abrasive tends to stabilize at $v=10\text{mm/s}$ by $v=6\text{m/s}$. When $v=10\text{m/s}$, abrasive wear rate tends to stabilize at $v=30\text{mm/s}$. And the wear rate increases with the increasing velocity, the difference is obvious. The wear rate increases significantly at the beginning of the simulation. Compared with the whole wear process, the wear rate is relatively small in the early stage of wear and shows an upward trend with the increasing of time step. As the relative sliding velocity becomes greater, the wear rate is more obvious, which is due to the impact of vibration on it.

After a period of wear, the corresponding abrasive wear has a relative increase. At the 750th step, we can see a significant difference. When the relative sliding velocity $v=6\text{m/s}$, the max wear depth $h=5.63\times 10^{-5}\text{mm}$. At $v=10\text{m/s}$, the max wear depth $h=8.88\times 10^{-5}\text{mm}$. The increase of the relative sliding velocity means that the friction and squeezing of the abrasive increases the wear quantity of the abrasive wear.

4.3. Effect of friction coefficient on abrasive wear

In the friction and wear process, the friction coefficient μ is a non-negligible parameter. It affects the result of wear directly. Take the friction coefficient of $\mu=0.30$, $\mu=0.45$ and $\mu=0.60$ for simulation analysis respectively, when the relative sliding velocity $v=10\text{m/s}$.

The difference of friction coefficient means that the degree of friction is different and has a corresponding effect on the interface temperature. The max temperature of the current sub-step is extracted every 10 steps. The interface temperature curve can be obtained at different friction coefficient, as shown in Figure 4.

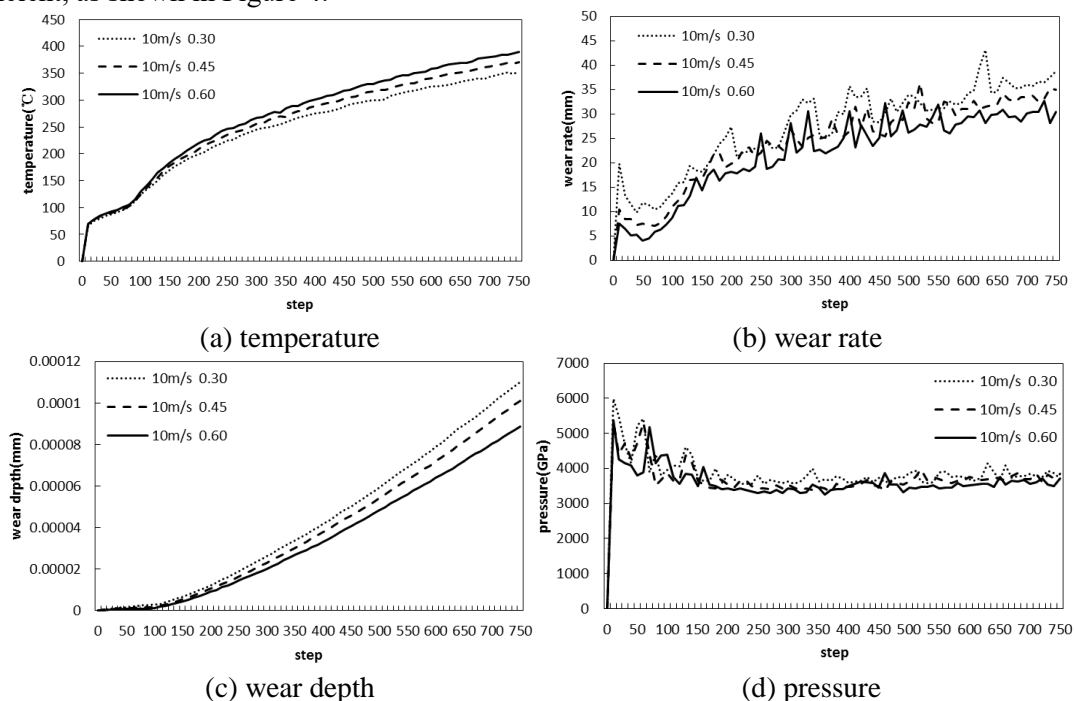


Figure 4. Chart of parameters with different friction coefficient.

Figure 4(a) shows the relationship between the different friction coefficient and the interface temperature. During the whole process it can be seen the interface temperature increases gradually with simulation steps. At the 750th step, the max interface temperature is at 352.928°C with the friction coefficient of 0.30. The friction coefficient $\mu=0.60$, the max interface temperature is at 389.344°C. The interface temperature increases as the coefficient of friction increasing, because the source of heat is sheared and squeezed between the materials during the wear process. The increase of the coefficient

friction causes the heat generated by friction between the abrasive and the brake pad, so the larger friction coefficient has a certain influence on the temperature rise.

Figure 4(b) and (c) show the relationship between the different friction coefficient and the wear rate as well as wear depth. It indicates the trend and the max of wear in the different friction coefficient respectively. From Figure 4(b) it could be found that when the friction coefficient becomes smaller, the wear rate is greater. It can be seen from Figure 4(c) that the max wear depth $h=1.10 \times 10^{-4}$ mm when $\mu=0.30$. The max wear depth $h=8.88 \times 10^{-5}$ mm at $\mu=0.60$. As the friction coefficient increasing, the wear quantity reduces accordingly. According to the Archard wear model, the wear is a function of the contact pressure and the relative sliding velocity. It can be seen from Figure 4(d) that the effect of the friction coefficient on the contact pressure is not obvious, but the amplification analysis can still find that the contact pressure decreases with coefficient increasing, thus the wear quantity decreases with the increase of friction coefficient.

5. Conclusions

This paper is based on abrasive wear theory of tribology, as well as the variation of the velocity and loads are considered in the micro friction and wear process. The Archard wear calculation model is modified. The micro finite element model of abrasive wear is established, the influence rules of relative sliding velocity and friction coefficient are analysed in the brake pad and disc. The simulation result shows that the wear is not stable at the initial stage, but the accumulation of wear depth tends to be moderate as time went on. The interface temperature rises with the increase of the relative sliding velocity. Although the larger friction coefficient elevates the interface temperature, the wear depth decreases with the influence of interface pressure and the relative sliding velocity.

Acknowledgments

The research work is supported by National Natural Science Foundation of China under Grant No. 51475066 and No. 51675075 and Natural Science Foundation of Liaoning Province under Grant No. 2015020114.

References

- [1] Zmago S, Kristoffer K and Tomaz K 2007 Friction behavior of sintered metallic brake pads on a C/C-SiC composite brake disc *J. Journal of the European Ceramic Society* **27** pp 1411–1417
- [2] Cho M H, Cho K H and Kim S.J 2005 The role of transfer layers on friction characteristics the sliding interface between friction materials against gray iron brake disks *J. Tribology Letters* **20** pp 101–108
- [3] Liu G, Wang Q and Ao Y 2002 Convenient Equations for modeling three dimensional thermo-mechanical asperity contacts *J. Tribology International* **35** pp 411–424
- [4] Bogdanovicha P N and Tkachu D V 2006 Temperature distribution over contact area and “hot spots” in rubbing solid contact *J. Tribology International* **39** pp 1355–1360
- [5] Straffelini G, Pellizzari M and Molinari A 2004 Influence of load and temperature on the dry sliding behavior of Al-based metal-matrix-composites against friction material *J. Wear* **256** pp 754–763
- [6] Eriksson M, Bergman F and Jacobson S 2002 On the nature of tribological contact in automotive brakes *J. Wear* **252** pp 26–36
- [7] Uyyuru R K, Surappa M K and Brusethaug S 2005 Effect of reinforcement volume fraction and size distribution on the tribological behavior of Al-composite/brake pad tribo-couple *J. Wear*, **257** pp 39–44
- [8] Zhou Z, He Y and Wang S 2014 Effect of Dimple Morphology on Line Contact Wear Resistance of Friction Pairs *J. Journal of Hunan University of Technology* **03** pp 24–29(in Chinses)
- [9] Archard J F 1953 Contact and rubbing of flat surfaces *J. Journal of Applied Physics* **24** pp 981–988